Configuration Optimization of Clamping Members of Frame-Supported Membrane Structures

M. Ohsaki[a,*], T. Nakajima[b], J. Fujiwara[c], F. Takeda[c]

[a] *Dept. of Architecture, Hiroshima University, Japan*
[b] *Dept. of Architecture and Architectural Engineering, Kyoto University, Japan*
[c] *Technical Research Center, Taiyo Kogyo Corporation, Japan*

Abstract

A method is presented for configuration optimization of frames that have specified properties on nodal displacements, stresses, and reaction forces against static loads. The conventional ground structure approach is first used for topology optimization. A feasible solution with small number of members satisfying all the design requirements except the stress constraints is obtained by assigning artificially small upper-bound displacement, or by penalizing the stiffness of a thin member. This way, the well-known difficulty in topology optimization under stress constraints is successfully avoided. The nodal locations and cross-sectional areas of the feasible solution are next optimized to obtain an approximate optimal configuration under stress constraints. The proposed method is applied to design of self-fastening clamping members for membrane structures modeled using frame elements. An optimization result is also presented for a clamping member that adjusts deformation of membrane by applying a clamping force with a vertically attached bolt.

Keywords: Membrane structure, Clamping member, Configuration optimization, Stress constraints

1. Introduction

Shape and topology optimization of continuum structures is a rather matured field of research [1–3], and there are many applications in various fields

*1-4-1, Kagamiyama, Higashi-Hiroshima 739-8527, Dept. of Architecture, Hiroshima University, Japan

Email address: ohsaki@hiroshima-u.ac.jp (M. Ohsaki)

of engineering including civil and architectural engineering [4–6]. The first author presented a method of optimizing shapes of beam flanges for maximizing the plastic energy dissipation under static deformation [7, 8]. This way, it is possible to optimize performances of mass-produced parts of building structures. However, topology optimization of continuum under stress constraints is still difficult, because of the design dependency of the optimization problem [9].

There are also many researches on simultaneous optimization of shape and topology, which is called *configuration optimization*, of trusses and frames [10–13]. Optimal topologies of trusses under constraints on global properties such as compliance and displacements can be easily obtained using the standard ground structure approach, where unnecessary members are removed through optimization from a highly-connected ground structure. However, even for trusses, there still exist several difficulties in problems under stress constraints [14–16], which are categorized as local constraints [17] that lead to existence of many thin members or elements; i.e., the number of members cannot be reduced effectively by simple application of the ground structure approach. In the most widely used SIMP (*solid isotropic microstructure with penalty* or *solid isotropic material with penalization*) approach [1, 18] to topology optimization of continua, an intermediate value of material density is penalized by assigning artificially small stiffness. Kim *et. al* [19] penalized the stiffnesses of the joints to obtain simple optimal topologies of frames. Takezawa *et al.* [20] formulated a frame optimization problem using a penalization parameter; however, they did not penalize the stiffness in the numerical examples. Therefore, to the authors' knowledge, there is no study on direct application of SIMP approach to topology optimization of frames.

Membrane structures are widely used for stadiums and arenas covering large space with lightweight membrane material [21, 22]. Membrane structures are generally connected to the boundary frames with clamping members as illustrated in Fig. 1. Since such devices are mass-products and have large portion of the total weight of the membrane structure, the total production cost can be reduced by optimizing the cross-sectional shapes of members. Furthermore, when external loads such as wind loads are applied to the membrane, its tensile force increases and the membrane sheet may detach from the clamping member prior to the fracture of membrane material. Therefore, the load resistance capacity of the membrane structure can be improved by optimizing the clamping members so that the clamping force increases as a result of increase of the tensile force of membrane.

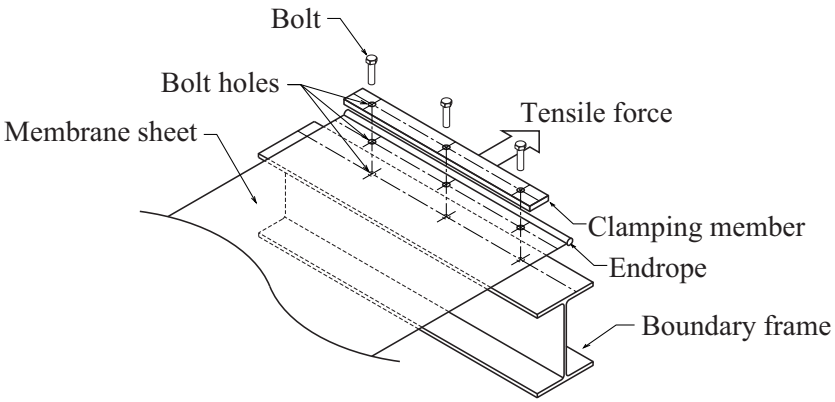

Figure 1: Illustration of a clamping member of a frame-supported membrane structure.

A structure that realizes the specified function utilizing its flexibility is called a compliant mechanism, which can be generated using structural optimization techniques [23–25]. However, those techniques cannot be directly applied to practical problems, because stress constraints should be satisfied by real-world structures.

In this paper, we first present a method for configuration optimization of general frames that have specified properties on nodal displacements, stresses, and reaction forces against static loads. We consider only static loads, because the regulations for design of structural parts in civil and architectural engineering are based on responses against static design loads. The ground structure approach is first used for topology optimization. A feasible solution with small number of members satisfying design requirements except the stress constraints is obtained by assigning artificially small upper-bound displacement, or by penalizing the stiffness of a thin member. The nodal locations and cross-sectional areas are next optimized for the feasible solution to obtain an approximate optimal configuration under stress constraints. This way, the well-known difficulty in topology optimization under stress constraints is successfully avoided.

The proposed method is applied to design of clamping members of frame-supported membrane structures. The clamping process of a membrane is illustrated in Fig. 2. In this process, temporary supports are attached first to the boundary frame of the structure along the boundary of the membrane sheet. To obtain reaction force from the boundary frame through

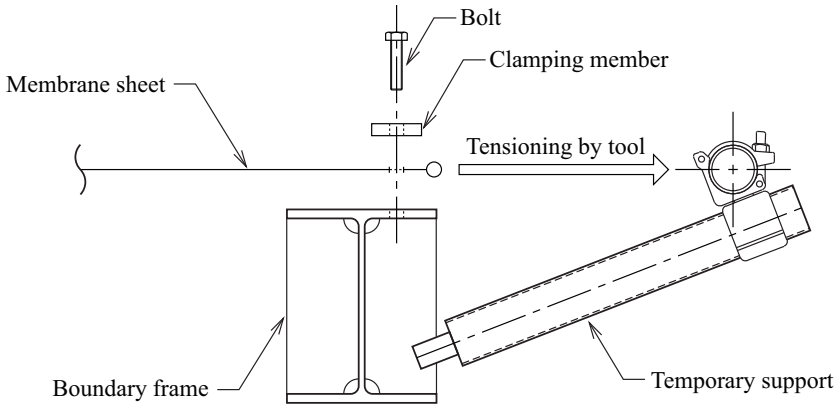

Figure 2: Construction process of a frame-supported membrane structure.

the temporary support, the membrane is pulled (tensioned) by using a tool until the preassigned holes of the membrane are located on the bolt holes of the boundary frame; then, the membrane is pressed to the frame using the clamping member and bolts. However, in this process, there exist the following difficulties:

1. Adjustment of tensile force of membrane is very difficult, because the holes are preassigned in the factory.
2. Temporary supports for obtaining reaction force through tensioning tools are needed in addition to the boundary frame.

In this paper, an optimization approach is presented to overcome these difficulties. The section of the clamping member is modeled as a frame that undergoes small elastic deformation. The objective function is the total structural volume, which is to be minimized, and the constraint is given for the clamping force against the membrane to obtain a self-fastening member. We also present an optimization result of a clamping member that enables us to adjust deformation of membrane by applying a clamping force through a vertically attached bolt.

2. Topology optimization of a self-fastening clamping member

2.1. Problem formulation

Simultaneous optimization of topology, cross-sectional areas of members, and nodal locations, which is simply called configuration optimization, is

carried out for a frame subjected to static loads. A two-step procedure is presented below to overcome difficulties in topology optimization under stress constraints.

The standard ground structure approach is used at the first step; i.e., unnecessary nodes and members are removed through optimization from the highly connected initial ground structure to obtain a frame with small number of members. The design variables are the cross-sectional areas $\boldsymbol{A} = (A_1, \ldots, A_m)$ of members, where m is the number of members in the ground structure. The cross-sectional properties such as the second moment of inertia and the section modulus are assumed to be functions of the cross-sectional area.

A constraint is given so that the maximum absolute value $|\sigma_i(\boldsymbol{A})|$ among the normal stresses of the ith member, evaluated at the two edges of two ends, does not exceed the specified upper bound σ^{U}. A lower bound R^{L} is also given for the reaction force $R(\boldsymbol{A})$ at the specified direction of a support. Then, the optimization problem for minimizing the total structural volume $V(\boldsymbol{A})$ is formulated as

$$\begin{aligned}
\text{P1}: \text{minimize} \quad & V(\boldsymbol{A}) && \text{(1a)}\\
\text{subject to} \quad & |\sigma_i(\boldsymbol{A})| \le \sigma^{\mathrm{U}}, \quad (i = 1, ..., m) && \text{(1b)}\\
& R(\boldsymbol{A}) \ge R^{\mathrm{L}} && \text{(1c)}\\
& \boldsymbol{A}^{\mathrm{L}} \le \boldsymbol{A} \le \boldsymbol{A}^{\mathrm{U}} && \text{(1d)}
\end{aligned}$$

where $\boldsymbol{A}^{\mathrm{L}} = (A_1^{\mathrm{L}}, \ldots, A_m^{\mathrm{L}})$ and $\boldsymbol{A}^{\mathrm{U}} = (A_1^{\mathrm{U}}, \ldots, A_m^{\mathrm{U}})$ are the lower and upper bounds for $\boldsymbol{A}$, respectively. Note that a small positive value is given for the lower-bound cross-sectional area to prevent instability of the frame during optimization process, and the member with $A_i = A_i^{\mathrm{L}}$ is removed after optimization.

An optimal topology satisfying constraints on stresses and a reaction force may be found by solving Problem P1, which is a standard nonlinear programming (NLP) problem. There exists a discontinuity in the gradient of the maximum stress in (1b), which can be avoided by assigning the upper- and lower-bound constraints for four edge-stresses of all members. However, we use the formulation (1b), because an optimal solution can be successfully found, as demonstrated in the numerical examples, using a gradient-based NLP algorithm with line search and a forward finite difference approach for evaluation of gradients. Note that the location and sign of maximum absolute value of stress in each member does not vary at the stage when the

optimization process converges; therefore, there is no difficulty for application of a finite-difference approach for gradient evaluation of the maximum absolute value of stress. Thus, the number of stress constraints is m, while it is $8m$ if upper and lower bounds are given for the four edge-stresses in each member.

It is well known in truss topology optimization that the number of members cannot be successfully reduced by using a conventional ground structure approach with an NLP algorithm, if stress constraints are considered [15, 16]. Therefore, we first carry out optimization, as follows, with a displacement constraint and without stress constraints:

$$\begin{aligned} \text{P2}: \text{minimize} \quad & V(\boldsymbol{A}) && \text{(2a)} \\ \text{subject to} \quad & |U(\boldsymbol{A})| \leq U^{\mathrm{U}} && \text{(2b)} \\ & R(\boldsymbol{A}) \geq R^{\mathrm{L}} && \text{(2c)} \\ & \boldsymbol{A}^{\mathrm{L}} \leq \boldsymbol{A} \leq \boldsymbol{A}^{\mathrm{U}} && \text{(2d)} \end{aligned}$$

where U^{U} is the upper bound for the absolute value of a specified displacement component $U(\boldsymbol{A})$. Problem P2 is first solved to obtain a topology with a small number of members. Then, Problem P1 is solved starting from the optimal solution of Problem P2 to obtain an approximate optimal topology under constraints on stresses and a reaction force.

In the numerical examples, the width of the section of each member is fixed, because the frame model represents a section of a clamping member; hence, the height is proportional to the cross-sectional area. Since the bending stiffness K is proportional to h^3 with a coefficient c as $K = ch^3$ for the solid rectangular section with the height h and constant width, the material is more efficiently used by a thick member than a thin member. In contrast, the axial stiffness is proportional to the height of the section. When the displacement bound becomes smaller, the members have larger heights and bending stiffness dominates over the axial stiffness. Consequently, a topology with small number of members can be obtained by assigning an artificially small upper-bound displacement.

Existence of thin members can also be avoided in a similar manner as SIMP approach for continuum topology optimization. Let p (≥ 1) denote a penalization parameter. An appropriately large value, e.g., the maximum value of A_i among all members in the optimal solution of Problem P2 with moderately large U^{U}, is denoted by $A^{\max}$. Then, the cross-sectional area A_i

is converted to a penalized value A_i^{P} using p as

$$A_i^{\mathrm{P}} = A_i^{\mathrm{L}} + (A^{\max} - A_i^{\mathrm{L}}) \left(\frac{A_i - A_i^{\mathrm{L}}}{A^{\max} - A_i^{\mathrm{L}}} \right)^p \tag{3}$$

For example, $A_i^{\mathrm{P}} = A_i$ if $p = 1$. In contrast, $A_i^{\mathrm{P}} = A_i^{\mathrm{L}} + (A_i^{\max} - A_i^{\mathrm{L}})/4$ if $(A_i - A_i^{\mathrm{L}})/(A_i^{\max} - A_i^{\mathrm{L}}) = 1/2$ and $p = 2$; i.e., in this case, the cross-sectional area is reduced by half if A_i^{L} is sufficiently small. Then, the optimization problem is formulated as

$$\begin{aligned} \mathrm{P3}: \text{minimize} \quad & V(\boldsymbol{A}) && \text{(4a)} \\ \text{subject to} \quad & |U(\boldsymbol{A}^{\mathrm{P}})| \leq U^{\mathrm{U}} && \text{(4b)} \\ & R(\boldsymbol{A}^{\mathrm{P}}) \geq R^{\mathrm{L}} && \text{(4c)} \\ & \boldsymbol{A}^{\mathrm{L}} \leq \boldsymbol{A} \leq \boldsymbol{A}^{\mathrm{U}} && \text{(4d)} \end{aligned}$$

where $\boldsymbol{A}^{\mathrm{P}} = (A_1^{\mathrm{P}}, \ldots, A_m^{\mathrm{P}})$. Note that the total structural volume is computed using $\boldsymbol{A}$, and the displacement and reaction force are computed using $\boldsymbol{A}^{\mathrm{P}}$. Therefore, $U(\boldsymbol{A}^{\mathrm{P}})$ and $R(\boldsymbol{A}^{\mathrm{P}})$ do not represent any physical values, because they are functions of the penalized cross-sectional areas.

It is seen from (3) that the stiffness of a member is artificially increased if A_i is larger than $A^{\max}$. Furthermore, convergence property of the NLP algorithm is deteriorated if too large value is given for p. It is shown in the following numerical examples that the parameter value between 1.5 and 2.0 can reach a good topology with small number of members without sacrificing convergence property.

Finally, the nodal locations as well as the cross-sectional areas are optimized to obtain the optimal configuration under constraints on stresses and a reaction force. The optimal solution of Problem P2 or P3 can be used as the ground structure with reduced number of members. Consequently, $\boldsymbol{A}$ and m denote the cross-sectional areas and the number of members of the ground structure with a reduced size. Let $\boldsymbol{X}$ denote the vector consisting of the variable components of the nodal coordinates. Then, the optimization

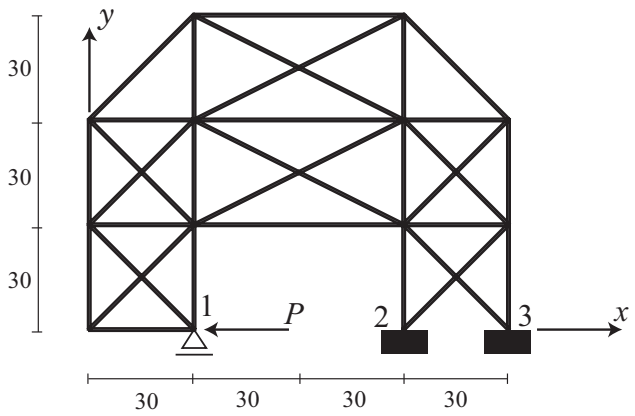

Figure 3: A frame model (Type 1).

problem is formulated as

$$\begin{aligned} \text{P4}: \text{minimize} \quad & V(\boldsymbol{A}, \boldsymbol{X}) && \text{(5a)} \\ \text{subject to} \quad & |\sigma_i(\boldsymbol{A}, \boldsymbol{X})| \leq \sigma^{\text{U}}, \quad (i = 1, ..., m) && \text{(5b)} \\ & R(\boldsymbol{A}, \boldsymbol{X}) \geq R^{\text{L}} && \text{(5c)} \\ & \boldsymbol{A}^{\text{L}} \leq \boldsymbol{A} \leq \boldsymbol{A}^{\text{U}} && \text{(5d)} \\ & \boldsymbol{X}^{\text{L}} \leq \boldsymbol{X} \leq \boldsymbol{X}^{\text{U}} && \text{(5e)} \end{aligned}$$

where $\boldsymbol{X}^{\text{L}}$ and $\boldsymbol{X}^{\text{U}}$ are the lower and upper bounds for $\boldsymbol{X}$, respectively.

In the following examples, optimization is carried out using the software library SNOPT Ver. 7.2 [26] utilizing sequential quadratic programming. The sensitivity coefficients are computed by using a finite difference approach. Since the problem under stress constraints has many local optimal solutions, a multistart strategy is used in the application of nonlinear programming [27, 28]; i.e., the best solution from ten different initial solutions is taken as an approximate optimal solution.

2.2. Numerical examples

We first find the cross-sectional shape of the clamping member that automatically clamps the membrane as the result of introducing tensile force to the membrane sheet. Consider a rigidly-jointed frame (Type 1) as shown in Fig. 3 as the ground structure, where the intersecting diagonal members are

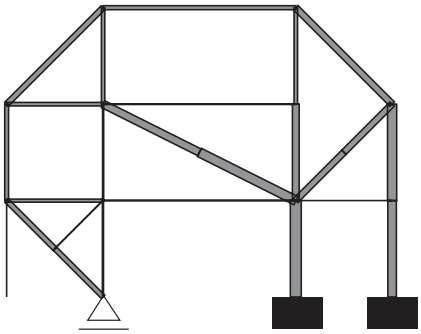

Figure 4: Optimal configuration of Type 1 for Problem P1 with stress constraints.

connected at the centers. The frame is supported with roller at support 1 and fixed at supports 2 and 3. The member is supposed to have solid rectangular section with the fixed width $b = 10$ mm. A load $P = 500$ N is applied in the negative x-direction at support 1. The reaction force R represents the vertical (positive y-directional) force at support 1; i.e., the device clamps the membrane if R is positive.

The elastic modulus of the members is 2.0×10^5 N/mm^2. The lower bound R^{L} for reaction force is 200 N, and the upper-bound stress σ^{U} is 200 N/mm^2. The cross-sectional areas of all 42 members are independent variables with lower bound $A_i^{\mathrm{L}} = 0.1$ mm^2, whereas different values of A_i^{U} are used for the optimization problems below. In the following, the units of length and force are mm and N, respectively. A uniform random number $0 \leq r_i < 1$ is generated to obtain the initial value of A_i as $50r_i + 1.0$.

Problem P1 is solved with the upper-bound cross-sectional area $A_i^{\mathrm{U}} = 200$; i.e., the upper-bound of height is $200/10 = 20$. The optimization result after removing the members with $A_i = A_i^{\mathrm{L}}$ is shown in Fig. 4, where the height of each member is drawn with real scale. Note that the reaction constraint is active as $R = R^{\mathrm{L}} = 200$, and the objective function value is $V = 1.1018 \times 10^4$. If all cross-sectional areas have the same value 100, then $R = -141.11$; i.e., the device should be pulled downward by the membrane sheet at support 1, which is not realistic; therefore, the direction of reaction force has been successfully reversed through optimization.

As is seen from Fig. 4, the number of members is not drastically reduced, because stress constraints should be satisfied in all members including very thin members. Therefore, Problem P2 is solved to obtain a topology with

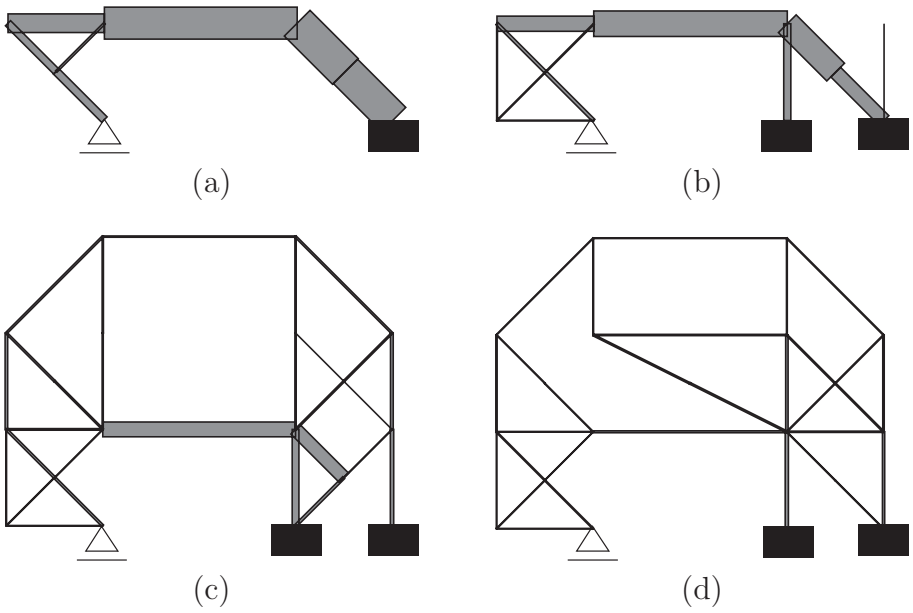

Figure 5: Optimal topology of Type 1 for Problem P2 with various values of U^{U}; (a) $U^{\mathrm{U}} = 0.01$, (b) $U^{\mathrm{U}} = 0.02$, (c) $U^{\mathrm{U}} = 0.04$, (d) $U^{\mathrm{U}} = 0.1$.

smaller number of members from the initial ground structure in Fig. 3. A large upper bound $A^{\mathrm{U}} = 1000$ is given to allow the existence of very thick members. The upper bound $U^{\mathrm{U}} = 0.1$ is given for the absolute value of the horizontal displacement of support 1.

The optimal topology is shown in Fig. 5(d), where the height of each member is scaled by 1/5. The optimal objective value is $V = 1.6781 \times 10^4$. As is seen from Fig. 5(d), there still exist many members that seem to be unnecessary. Therefore, we assign smaller upper-bound displacement to allow larger structural volume and cross-sectional areas. The optimal solution for $U^{\mathrm{U}} = 0.01$ is shown in Fig. 5(a), where $V = 6.7593 \times 10^4$ and the height of each member is scaled by 1/5. The solutions for $U^{\mathrm{U}} = 0.02$ and 0.04 are also shown in Figs. 5(b) and (c), respectively. We can confirm from Figs. 5(a)–(d) that the number of members decreases and the heights of existing members increase as the displacement constraint becomes tight.

The total structural volume V and number of members n^{opt} of optimal topology for various values of U^{U} are listed in Table 1. We can confirm that a solution with smaller n^{opt} and larger V is obtained as U^{U} is decreased.

Table 1: Total structural volume V and number of members n^{opt} of optimal topologies of Type 1 for Problem P2 with various values of U^{U}.

U^{U}	V $(\times 10^4)$	n^{opt}
0.1	1.6782	30
0.09	1.8513	30
0.08	2.3396	27
0.07	2.3516	30
0.06	2.7289	30
0.05	3.2310	28
0.04	3.8090	28
0.03	4.6826	29
0.02	5.0352	12
0.01	6.7593	7

However, the maximum height of the members in Fig. 5(a) for $U^{\mathrm{U}} = 0.01$ is 56.439, which is unrealistic in comparison to the dimension of the frame. Furthermore, stress constraints should be satisfied for practical application. Hence, the displacement bound is conceived as an artificial parameter for controlling the number of members in a frame that satisfies design requirements except the stress constraints.

Optimal solutions are also found for Problem P3 with various values of the penalization parameter p. The displacement bound is $U^{\mathrm{U}} = 0.1$, and the maximum cross-sectional area 49.226 of the optimal solution in Fig. 5(d) is assigned for $A^{\max}$. Figs. 6(a)–(d) show the solutions for $p = 1.4$, 1.5, 1.7, and 2.0, respectively, where the height of each member is scaled by 1/5. The total structural volume V and number of members n^{opt} of optimal topologies for various values of p are listed in Table 2. As is seen from Figs. 6(a)–(d) and Table 2, a solution with smaller number of members is obtained by increasing p. However, there is no correlation between p and V, because the stiffness is artificially increased for a member with $A_i > A^{\max}$, while it is decreased for $A_i < A^{\max}$.

We next solve Problem P4 using the solution in Fig. 5(a) as the initial ground structure with reduced number of members. Each member in Fig. 5(a) is divided into shorter members to obtain a smoothly curved frame. The vertical coordinates of nodes except the supports are also considered

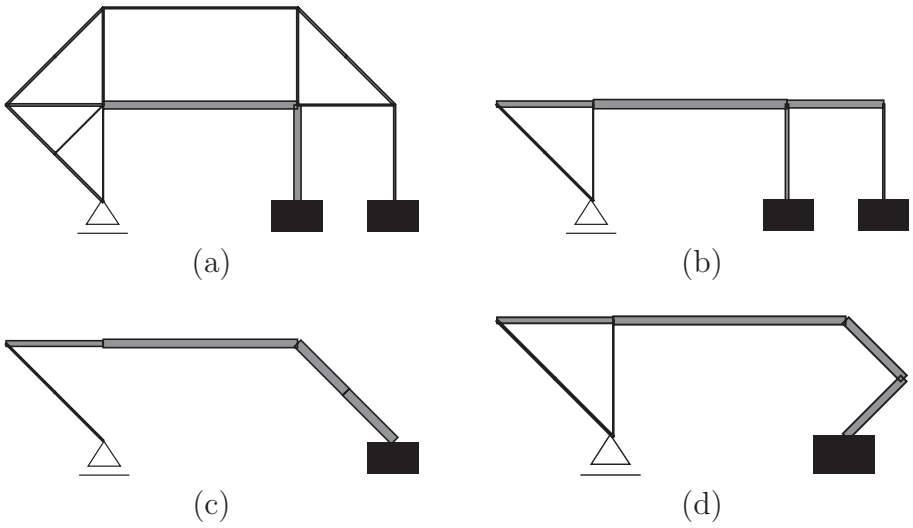

Figure 6: Optimal topologies of Type 1 for Problem P3 with various values of p; (a) $p = 1.4$, (b) $p = 1.5$, (c) $p = 1.7$, (d) $p = 2.0$.

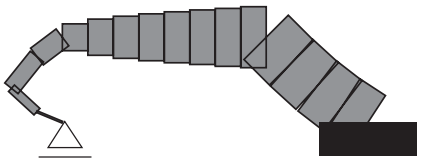

Figure 7: Optimal solution of Type 1 for Problem P4 with stress constraints with variable nodal locations.

as design variables. Let Y_i^0 denote the y-coordinate of the ith node of the initial frame obtained by sub-division of the frame in Fig. 5(a). The upper and lower bounds for Y_i are given as $Y_i^0 + 5$ and $Y_i^0 - 5$, respectively. Note that rather strict bounds are given to avoid an optimal shape with small height, because the endrope for the membrane sheet should be contained in the clamping member.

Fig. 7 shows the optimal shape with real scale, where $V = 1.7082 \times 10^4$. Fig. 8 shows the deformed shape with magnification factor 20 for the nodal displacement. As is seen, only the nodes near support 1 move in the horizontal direction; thus, a vertical compressive force is applied from the frame to the support, and, accordingly, the clamping force increases as

Table 2: Total structural volume V and number of members n^{opt} of optimal topologies of Type 1 for Problem P3 with various values of p.

p	V $(\times 10^4)$	n^{opt}
1.0	1.6782	30
1.1	1.8149	30
1.2	1.9353	28
1.3	2.0391	28
1.4	2.0892	16
1.5	1.8657	8
1.6	2.1156	9
1.7	1.7690	6
1.8	1.7057	8
1.9	1.4470	9
2.0	1.4740	7

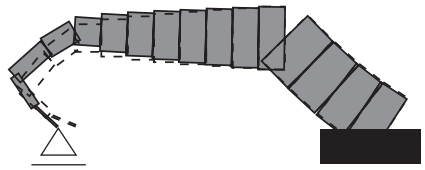

Figure 8: Deformed shape of optimal solution of Type 1 for Problem P4 with stress constraints with variable nodal locations; dotted line: undeformed shape.

the tensile force of the membrane sheet increases. From this result, we can construct a self-fastening clamping member as illustrated in Fig. 9.

Finite element (FE) analysis is carried out using ABAQUS 6.9.2 [29] for verification of the results obtained by the frame model. The FE-meshes of the section modeled as a plate are shown in Fig. 10(a), and the shell elements S4R (quadratic) and S3R (triangular) are used. The boundary of the plate is defined by extrapolating the upper and lower edges of the beam elements of the frame model. The plate is supported by roller at point A, and fixed at the nodes along line BC. The deformed configuration with magnification factor 10 is shown in Fig. 10(b) with the contour lines for the von Mises stress. The maximum von Mises stress is 140.23, which is less than the upper-bound stress 200 in the frame optimization problem. The vertical reaction force at

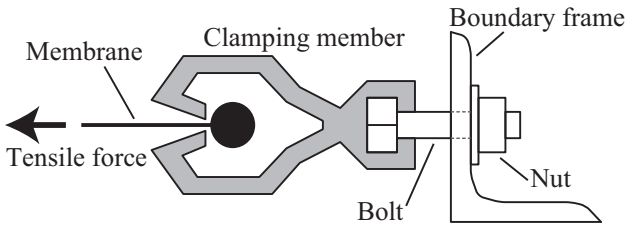

Figure 9: Illustration of the section of a self-fastening clamping member.

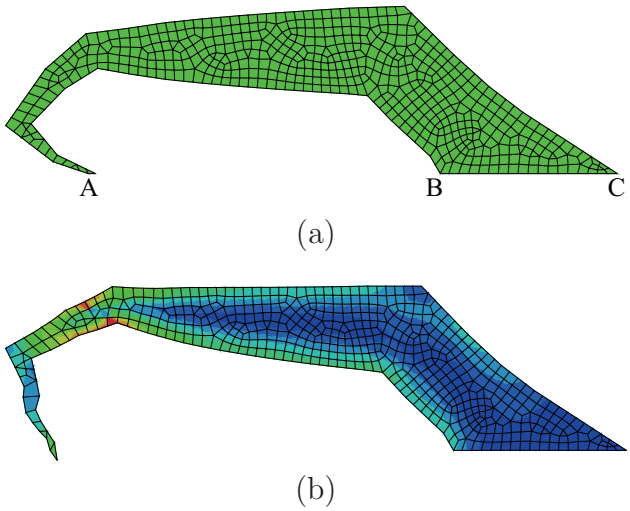

Figure 10: Deformation and contour lines of von Mises stress by FE-analysis for verification of optimal solution of Type 1; (a) undeformed shape, (b) deformed shape.

the roller support is 256.95, which is larger than the lower bound 200. Hence, the section satisfying the design requirements has been successfully found.

3. Topology optimization of a clamping member with a tension adjustment bolt

3.1. Problem formulation

In Sec. 2, we presented a method for generating a clamping member that can automatically fasten the membrane sheet as the tensile force is increased. However, for application to the practical design of membrane structures, it is more desirable if the tensile force can be adjusted through additional forces

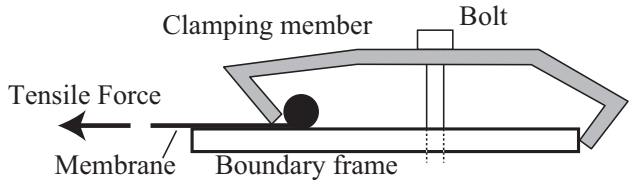

Figure 11: Illustration a clamping member with tension adjustment bolt.

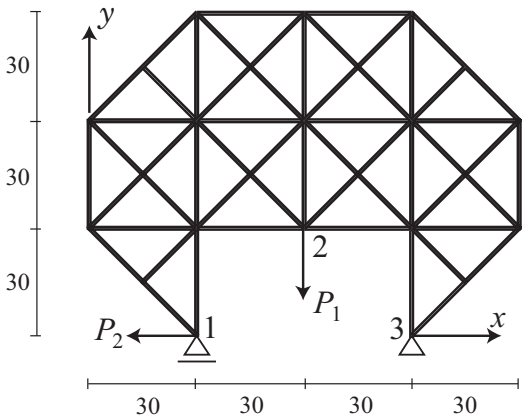

Figure 12: A frame model (Type 2).

to the clamping member as illustrated in Fig. 11. Therefore, we next consider a problem with two loading conditions. The section is modeled by a frame, and its initial ground structure is as shown in Fig. 12. The load P_1 is first applied at node 2 by the vertical bolt to pull the membrane for adjustment of the tensile force. Then, the vertical location of node 2 is fixed and the second load P_2 representing the tensile force of the membrane sheet is applied at support 1.

Let $U^{(1)}$ and $U^{(2)}$ denote the x-directional displacements of support 1 in Fig. 12 under specified static loads P_1 and P_2, respectively. We first minimize the total structural volume V without stress constraint to obtain a frame with small number of members. The lower bound $U^{(1)\mathrm{L}}$ (> 0) is given to ensure capacity of adjustment by the bolt, and the lower bound $U^{(2)\mathrm{L}}$ (< 0) is given for generating a frame with enough stiffness. Then the optimization problem

Figure 13: Optimal solution of Type 2 for Problem P5 under displacement constraint.

is formulated as follows:

$$\begin{aligned} \text{P5}: \text{minimize} \quad & V(\boldsymbol{A}) && \text{(6a)} \\ \text{subject to} \quad & U_1^{(1)}(\boldsymbol{A}) \geq U^{(1)\mathrm{L}} && \text{(6b)} \\ & U_1^{(2)}(\boldsymbol{A}) \geq U^{(2)\mathrm{L}} && \text{(6c)} \\ & \boldsymbol{A}^{\mathrm{L}} \leq \boldsymbol{A} \leq \boldsymbol{A}^{\mathrm{U}} && \text{(6d)} \end{aligned}$$

The optimal solution of Problem P5 is used as the new ground structure with small number of members. Since the number of members need not be reduced anymore, the displacement $U_1^{(1)}$ against P_1 can be directly maximized to obtain a good capacity of adjustment of membrane forces. Hence, we assign the stress constraints for both the states under P_1 only and under application of P_2 after constraining node 2, and solve the following problem adding the nodal coordinates $\boldsymbol{X}$ as variables:

$$\begin{aligned} \text{P6}: \text{maximize} \quad & U_1^{(1)}(\boldsymbol{A}, \boldsymbol{X}) && \text{(7a)} \\ \text{subject to} \quad & U_1^{(2)}(\boldsymbol{A}, \boldsymbol{X}) \geq U^{(2)\mathrm{L}} && \text{(7b)} \\ & |\sigma_i^{(1)}(\boldsymbol{A}, \boldsymbol{X})| \leq \sigma^{\mathrm{U}}, \quad (i = 1, \ldots, m) && \text{(7c)} \\ & |\sigma_i^{(1)}(\boldsymbol{A}, \boldsymbol{X}) + \sigma_i^{(2)}(\boldsymbol{A}, \boldsymbol{X})| \leq \sigma^{\mathrm{U}}, \quad (i = 1, \ldots, m) && \text{(7d)} \\ & \boldsymbol{A}^{\mathrm{L}} \leq \boldsymbol{A} \leq \boldsymbol{A}^{\mathrm{U}} && \text{(7e)} \\ & \boldsymbol{X}^{\mathrm{L}} \leq \boldsymbol{X} \leq \boldsymbol{X}^{\mathrm{U}} && \text{(7f)} \end{aligned}$$

where $\sigma_i^{(1)}$ and $\sigma_i^{(2)}$ are the stresses of member i against P_1 and P_2, respectively.

3.2. Numerical examples

Consider a frame as shown in Fig. 12. The load $P_1 = 300$ is first applied in negative y-direction at node 2. Then the y-directional displacement is

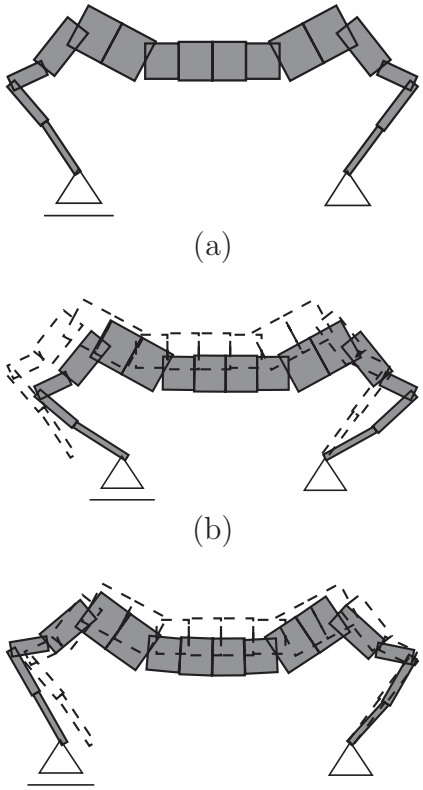

Figure 14: Optimal solution of Type 2 for Problem P6 under stress constraints; (a) undeformed shape, (b) deformed shape magnified by 10 under P_1; dotted line: undeformed shape, (c) deformed shape magnified by 10 under P_2 after constraining node 2; dotted line: undeformed shape.

fixed at node 2, and the load $P_2 = 500$ is applied in negative x-direction at support 1. Initial solutions are generated in the same manner as the example in Sec. 2.

The solution of Problem P5 scaled by 1/5 for $U^{(1)\mathrm{L}} = 0.1$, $U^{(2)\mathrm{L}} = -0.01$, and $A_i^{\mathrm{U}} = 200$ for all members is shown in Fig. 13, which has sufficiently small number of members. Problem P6 is next solved after subdivision of members, where the y-coordinates of nodes except the supports are also chosen as design variables, and their initial values and bounds are given in the same manner as the example in Sec. 2. The optimal solution for $\sigma^{\mathrm{U}} = 300$

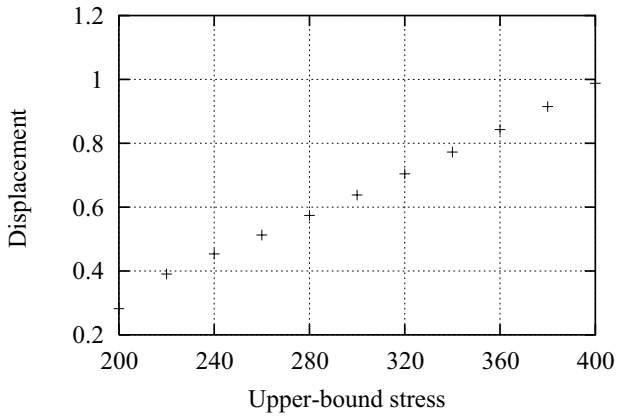

Figure 15: Relation between upper-bound stress and displacement.

is shown in Fig. 14(a) with the real scale for the heights of members. The deformed shape under P_1 is shown in Fig. 14(b). We can see from Fig. 14(b) that the distance between the two supports decreases as the center node is displaced downward. Fig. 14(c) shows the state under P_2 after constraining vertical displacement at node 2.

Fig. 15 shows the relation between the upper-bound stress σ^{U} and the displacement $U^{(1)}$ of the optimal solution of P6. It can be confirmed from Fig. 15 that we can have larger deformation if the stress constraints are relaxed.

FE-analysis is carried out for verification of the result in Fig. 14 obtained by the frame model for $\sigma^{\mathrm{U}} = 300$. The FE-meshes in Fig. 16(a) are generated in the same manner as those in Sec. 2. The plate is supported by roller at point A and pin at point B. The deformed configuration under P_1 with magnification factor 10 is shown in Fig. 16(b). The contour lines show the von Mises stress. The horizontal displacement of the support is 0.57424. The maximum von Mises stress is 162.09, which is less than the upper bound. Fig. 16(c) shows the deformed configuration after application of P_2. The maximum von Mises stress is 253.62, which is less than the upper bound. Hence, the section satisfying the design requirements has been successfully found.

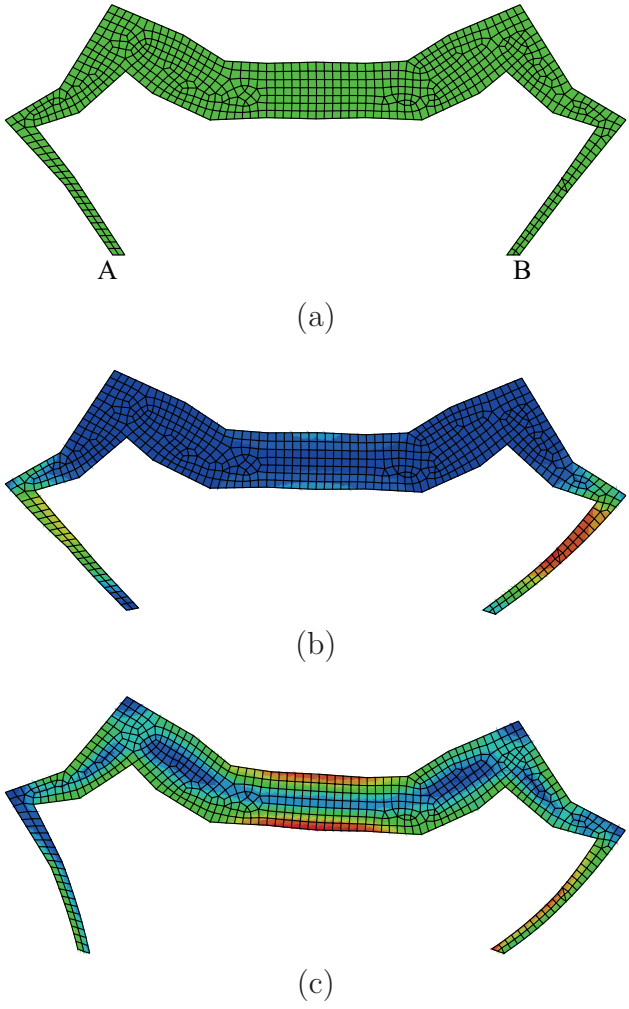

Figure 16: Deformation and contour lines of von Mises stress by FE-analysis for verification of optimal solution of Type 2; (a) undeformed shape, (b) deformed shape magnified by 10 under P_1, (c) deformed shape magnified by 10 under P_2 after constraining node 2.

4. Conclusions

A two-stage approach has been presented for configuration optimization of frames under constraints on stresses, reaction force, and displacement against static loads. It has been shown that the optimal topology has many members if stress constraints are assigned to all members. This result is similar to the truss topology optimization under stress constraints. Therefore, a problem

without stress constraint and with artificial displacement constraint is first solved in the proposed two-stage approach.

A solution with small number of members can be found if very tight bound for the displacement and very large upper bounds for cross-sectional areas are given, because the bending stiffness is proportional to the cubic power of the height, and the axial stiffness is proportional to the height of a member with solid section, and, accordingly, a member with larger height is more efficient than that with smaller height when bending deformation dominates over axial deformation. The stiffness of a member with small height can also be penalized using the approach similar to the SIMP method for continuum topology optimization.

The frame with small number of members obtained in the first stage has been further optimized under stress constraints after sub-division of members, where the vertical coordinates of nodes are also considered as design variables. This way, the well-known difficulty in topology optimization under stress constraints is successfully avoided.

As an application of the proposed approach, configuration optimization has been carried out to obtain a self-fastening clamping member of a frame-supported membrane structure. The total structural volume is minimized under constraint on the reaction so that the clamping force increases as the result of increasing membrane tensile force. A shape of the device that pulls the membrane efficiently by applying vertical force through a bolt can also be found using the proposed two-stage approach. This way, the total weight of a frame-supported membrane structure can be reduced, and the clamping force and the tension force can be maintained through optimization.

Acknowledgment
Financial support by Nohmura Foundation for Membrane Structure's Technology is gratefully acknowledged.

References

[1] M. P. Bendsøe, O. Sigmund, Topology Optimization: Theory, Methods and Applications, Springer, Berlin, 2003.

[2] A. Kaveh, B. Hassani, S. Shojaee, S. M. Tavakkoli, Structural topology optimization using ant colony methodology, Eng. Struct. 30 (2008) 2559–2565.

[3] X. Huang, Y. M. Xie, Topology optimization of nonlinear structures under displacement loading, Eng. Struct. 30 (2008) 2057–2068.

[4] N. Lagaros, L. D. Psarras, M. Papadrakakis, G. Kokossalakis, Optimum design of steel structures with web opening, Eng. Struct. 30 (2008) 2528–2537.

[5] A. R. Mijar, C. Swan, J. S. Arora, I. Kosaka, Continuum topology optimization for concept design of frame bracing system, J. Struct. Eng. 124 (5) (1998) 541–550.

[6] H.-G. Kwak, S.-H. Noh, Determination of strut-and-tie models using evolutionary structural optimization, Eng. Struct. 28 (2006) 1440–1449.

[7] P. Pan, M. Ohsaki, H. Tagawa, Shape optimization of H-beam flange for maximum plastic energy dissipation, J. Struct. Eng. 133 (8) (2007) 1176–1179.

[8] M. Ohsaki, H. Tagawa, P. Pan, Shape optimization of reduced beam section for maximum plastic energy dissipation under cyclic loads, J. Const. Steel Res. 65 (2009) 1511–1519.

[9] M. Bruggi, On an alternative approach to stress constraints relaxation in topology optimization, Struct. Multidisc. Optim. 36 (2008) 125–141.

[10] H. Rahamia, A. Kaveh, Y. Gholipoura, Sizing, geometry and topology optimization of trusses via force method and genetic algorithm, Eng. Struct. 30 (2008) 2360–2369.

[11] H. Fredricson, T. Johansen, A. Klarbring, J. Petersson, Topology optimization of frame structures with flexible joints, Struct. Multidisc. Optim. 25 (2003) 199–214.

[12] M. P. Saka, Optimum topological design of geometrically nonlinear single layer latticed domes using coupled genetic algorithm, Comput. Struct. 85 (2007) 1635–1646.

[13] M. Ohsaki, Optimization of Finite Dimensional Structures, CRC Press, Boca Raton, FL, 2010.

[14] M. Stolpe, K. Svanberg, A note on stress-constrained truss topology optimization, Struct. Multidisc. Optim. 25 (2003) 62–64.

[15] M. Ohsaki, N. Katoh, Topology optimization of trusses with stress and local constraints on nodal stability and member intersection, Struct. Multidisc. Optim. 29 (2005) 190–197.

[16] G. Cheng, X. Guo, ε-relaxed approach in structural topology optimization, Struct. Opt. 13 (1997) 258–266.

[17] P. Duysinx, M. P. Bendsøe, Topology optimization of continuum structures with local stress constraints, Int. J. Numer. Meth. Eng. 43 (1998) 1453–1478.

[18] G. I. N. Rozvany, M. Zhou, T. Birker, Generalized shape optimization without homogenization, Struct. Optim. 4 (1992) 250–252.

[19] M.-J. Kim, G.-W. Jang, Y. Y. Kim, Application of a ground beam-joint topology optimization method for multi-piece frame structure design, J. Mech. Design 130 (8) (2008) Paper–081401.

[20] A. Takezawa, S. Nishiwaki, K. Izui, M. Yoshimura, Structural optimization based on topology optimization techniques using frame elements considering cross-sectional properties, Struct. Multidisc. Optim. 34 (2007) 41–60.

[21] J.-Y. Kim, J.-B. Lee, A new technique for optimum cutting pattern generation of membrane structures, Eng. Struct. 24 (6) (2002) 745–756.

[22] B. Maurin, R. Motro, The surface stress density method as a form-finding tool for tensile membranes, Eng. Struct. 20 (8) (1998) 712–719.

[23] M. I. Frecker, G. K. Ananthasuresh, S. Nishiwaki, N. Kikuchi, S. Kota, Topological synthesis of compliant mechanisms using multi-criteria optimization, J. Mech. Design 119 (2) (1997) 238–245.

[24] O. Sigmund, On the design of compliant mechanisms using topology optimization, Mech. Struct. & Mach. 25 (4) (1997) 493–524.

[25] M. Ohsaki, S. Nishiwaki, Shape design of pin-jointed multistable compliant mechanism using snapthrough behavior, Struct. Multidisc. Optim. 30 (2005) 327–334.

[26] P. E. Gill, W. Murray, M. A. Saunders, SNOPT: An SQP algorithm for large-scale constrained optimization, SIAM J. Optim. 12 (2002) 979–1006.

[27] H. Kim, R. T. Haftka, W. H. Mason, L. T. Watson, B. Grossman, Probabilistic modeling of errors from structural optimization based on multiple starting points, Optim. Eng. 3 (2002) 415–430.

[28] P. Pan, M. Ohsaki, T. Kinoshita, Constraint approach to performance-based design of steel moment-resisting frames, Eng. Struct. 29 (2007) 186–194.

[29] ABAQUS Ver. 6.9.2 Documentation, ABAQUS Inc., 2010.